Experiment Study on Optical Lattice Clock of Strontium at NTSC

Tian Xiao[1,2] Xu Qinfang[1] Yin Mojuan[1] Kong Dehuan[1] Wang Yebing[1]
Lu Benquan[1,2] Liu Hui[1,2] Ren Jie[1] Chang Hong[1]

[1] *Key Laboratory of Time and Frequency Primary Standards of Chinese Academy of Sciences, National Time Service Center, Xi, an, Shaanxi* 710600, *China*

[2] *University of Chinese Academy of Sciences, Beijing* 100049, *China*

Abstract The accuracy and stability of optical clocks has achieved 10^{-18} level currently. The progress on the optical lattice clocks of Strontium (Sr) atoms at National Time Service Center is presented. ^{88}Sr, which has the highest natural abundance in four isotopes of Sr, is cooled on the basis of transitions $(5s5s)^1S_0$—$(5s5p)^1P_1$ and $(5s5s)^1S_0$—$(5s5p)^3P_1$. In order to cancel the effect of Doppler shift and recoil shift these cold atoms are trapped in the optical lattice. However, the optical lattice where atoms are trapped can make the energy level shift, called A. C. Stark shift. The "magic" wavelength for clock transition $(5s5s)^1S_0$—$(5s5p)^3P_0$ can make the same Stark light-shift for both of them, being value 813.4 nm. Then those cold ^{88}Sr atoms are confined in a 1-D optical lattice constituted by the laser outputting from an amplified diode laser, operating on the "magic" wavelength 813nm. Consequently, the lifetime of atoms in 1-D optical lattice is measured and the value is 270 ms. The temperature and the number are about 3.5 μK and 1.2×10^5 respectively. Atoms confined in the optical lattice can provide a long interrogation time for probing the clock transition, furthermore make the foundation for developing the optical lattice clock of Sr atoms.

Key words quantum optics; time and frequency standard; cold atom; optical lattice; clock transition

OCIS codes 020.3320; 020.7010; 140.2020; 300.2530

国家授时中心锶原子光钟的实验研制进展

田 晓[1,2] 徐琴芳[1] 尹默娟[1] 孔德欢[1] 王叶兵[1] 卢本全[1,2] 刘 辉[1,2]
任 洁[1] 常 宏[1]

[1] 中国科学院国家授时中心时间频率基准重点实验室,陕西 西安 710600

[2] 中国科学院大学,北京 100049

摘要 目前光钟的稳定度和不确定度均已进入 10^{-18} 量级。介绍了中国科学院国家授时中心的锶原子光晶格钟的研究情况。以锶原子四种同位素中自然丰度最大的^{88}Sr 为研究对象,依次实现了^{88}Sr 的一级冷却和二级冷却。为消除一阶多普勒频移和反冲频移对冷原子运动的影响,充分发挥原子极窄钟跃迁谱线线宽的优点,冷原子被囚禁于光晶格中。而由光晶格导致的原子能级频移的问题可被"魔术"波长解决,对锶原子光钟,光晶格波长为813.4 nm。实验中采用功率放大的半导体激光器输出"魔术"波长激光,通过一维驻波光场搭建将^{88}Sr 装载进一维光晶格中。测量得到囚禁于光晶格中的冷原子寿命为 270 ms,温度为 3.5 μK,数目为 1.2×10^5。光晶格囚禁为下一步的钟跃迁信号提供了较长的探测时间并且有利于获得极窄线宽的钟跃迁谱线,因此是光钟研制中很重要的一步。

关键词 量子光学;时间频率基准;冷原子;光晶格;钟跃迁

中图分类号 O562.5;O431.2 **文献标识码** A

doi: 10.3788/AOS201535.s102001

收稿日期: 2015-01-22; **收到修改稿日期**: 2015-03-03

基金项目: 国家自然科学基金(61127901,11474282)

作者简介: 田晓(1984—),女,博士研究生,主要从事时间频率基准方面的研究。E-mail:tianxiao@ntsc.ac.cn

导师简介: 常宏(1977—),男,研究员,博士生导师,主要从事原子光学及时间频率基准方面的研究。E-mail:changhong@ntsc.ac.cn(通信联系人)

1 Introduction

Owing to high operational frequency, time and frequency standard based on optical transitions has made substantial progress over the last few years[1-6]. In 2010, National Institute of Standards and Technology realized the Al^+ optical clock with uncertainty 8.6×10^{-18} at the first time[7]. In 2014, Joint Institute for Laboratory Astrophysics achieved the accuracy of 6.4×10^{-18}, low instability 3×10^{-18} (sampling time about 1000s) of the ^{87}Sr optical lattice clock[8].

It is worth noting that the optical lattice is utilized in optical clocks where neutral atoms are confined in the Lamb-Dicke regime. This tight atomic confinement is a specific and original feature of optical lattice clock, greatly different from the previous generation of clocks[9-12]. For this new clock, atoms are trapped so their motions, which is known to be affected on the accuracy of the measurement, are ideally controlled. Besides, a large number of atoms contribute to the stability of optical lattice clocks. Although confinement of single ions enables long interaction time and the Doppler-free as well as the recoil-free absorption, owing to be limited by quantum projection noise, frequency stabilities of ion clocks are degraded ultimately[13-14]. There are advantages for developing optical lattice clocks. However, atomic levels trapped in an optical lattice are shifted by A. C. Stark effect, which lowers the capability of the optical clock finally. For the magnitude of the shift, the value of several tens of kHz is equivalent to about 10^{-10} for optical frequency[15]. The "magic wavelength" which can makes the clock transitions (the ground state and the excited state) has the same shift, is proposed and analyzed theoretically by the H Katori's group of Tokyo university at the first time[16].

In this paper, the progress on the optical lattice clocks of Sr atoms at National Time Service Center (NTSC) is described. The experiment of bosonic atoms ^{88}Sr is introduced. In part 2, the experiment of cooling ^{88}Sr by two-stage is reported, including the $(5s5s)^1S_0$—$(5s5p)^1P_1$ cooling and $(5s5s)^1S_0$—$(5s5p)^3P_1$ cooling. In part 3, the principle about optical lattice is analyzed briefly. Based on the analysis, the trapping depth and frequency are calculated theoretically for our experiment and then the experiment of one-dimensional (1-D) optical lattice is realized. The intensity noise of the lattice laser is also studied. Part 4 is the conclusion of our Sr optical lattice clock. Based on trapped atoms in the 1-D optical lattice, the clock transition $(5s5s)^1S_0$—$(5s5p)^3P_0$ is studied.

2 Preparation of cold Sr atoms

Sr located in Group Ⅱ of the periodic table has two valence electrons, which is promising candidate for development of the optical time and frequency standard. The two valence electrons create a rich mixture of electronic states, neatly divided into spin singlet and spin triplet states. For neutral Sr, the doubly-forbidden, spin induced $^1S_0$—$^3P_0$ transition in ^{87}Sr has the potential for its very narrow line-width of 1 mHz. The natural abundance of ^{88}Sr is one order of magnitude higher than that of ^{87}Sr and ^{88}Sr also simpler to be cooled than ^{87}Sr. So the ^{88}Sr optical clock is studied in the first place and then the ^{87}Sr optical clock.

In NTSC, the experiment of cooling and trapping Sr atoms is carried out in an extremely ideal vacuum environment with 10^{-7} Pa. Figure 1 shows the experimental apparatus. At room temperature, Sr atoms show a form of solid. Thus atoms are heated to be steamed in an oven. The temperature of the oven is set at about 810K and then the atomic steam pass through a collimator, composed of more than one thousand hollow tubes whose diameter is 0.2 mm and length is 8.0 mm. After that an atomic beam is formed with a spread angle smaller than 40 mrad. Coming out from the collimator, 2-dimension cooling is carried out here in order to achieve a higher collimation.

The cold atoms are realized by two steps in the MOT chamber. The dipolar energy-level transition $(5s5s)^1S_0$—$(5s5p)^1P_1$ whose corresponding wavelength is 461nm with natural line-width of 32MHz, is used for the first-stage cooling. For the second-stage cooling, the transition $(5s5s)^1S_0$—$(5s5p)^3P_1$ is used,

whose corresponding wavelength is 689nm with natural line-width of only 7.6kHz. The 461nm cooling is described in our previous work in detail[17-18]. The repumping lasers 707nm and 679nm locked[19-20] are added here to increase the number of cold atoms. After 461nm cooling, the cold atoms is obtained (also called Blue MOT) with temperature 5mK and the number at the level of 10^8 approximately.

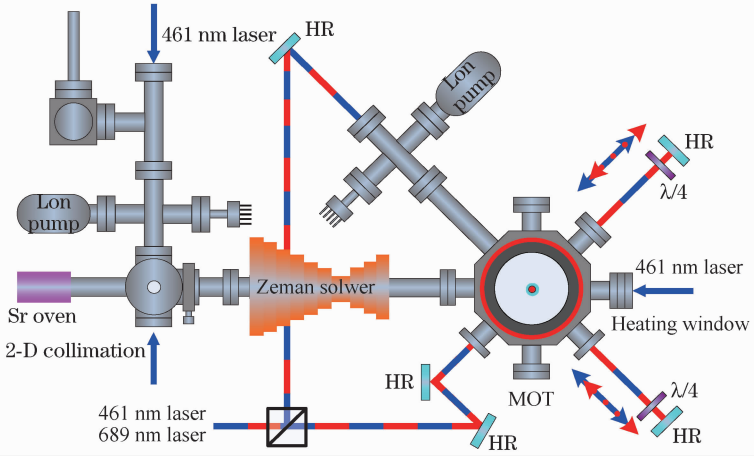

Fig. 1　Experimental setup of cooling Sr atoms

For the narrow 689nm cooling with line-width 7.6 kHz, a narrow line-width laser is needed. In our experiment, the line-width of diode laser resource 689nm is narrowed by the Pound-Drever-Hall (PDH) technology[21]. According to the beat signal between the two same narrow line-width systems of 689nm laser, its line-width is obtained and it is 290Hz, with its stability of 4.4×10^{-14}@16s. Immediately, after the blue MOT is turned off, the narrow line-width 689nm is turned on. Firstly, the laser is modulated with 50kHz and at the same time the B-field gradient is turned down from 50 Gs/cm to 3Gs/cm. After the broadband cooling accomplished, the modulation is cut off and B-field gradient is changed from 3Gs/cm to 10Gs/cm. A lower temperature and smaller volume of atoms are produced in the process of single frequency cooling than the broadband one. Atoms are cooled further by narrow line-width 689 nm which is called Red MOT, too. An Electronic Multiple Charge Coupled Device (EMCCD) is utilized to capture the image of cold atoms, shown in figure 2.

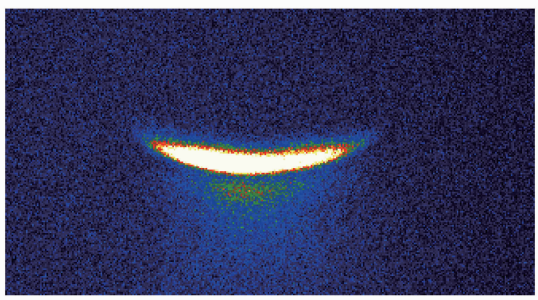

Fig. 2　Image of μK cold ^{88}Sr atoms captured by an EMCCD

A method, time of flight (TOF)[22], is used here to measure the temperature of cold atoms, which can be estimated by the equation

$$T_{\mathrm{atom}}=\frac{m}{4k_{\mathrm{B}}t^2}(\sigma_t^2-\sigma_0^2), \tag{1}$$

Where m is the mass of Sr atom, k_{B} is Boltzmann's constant, t is the falling time, σ_0 is the atomic initial Gaussian radius, σ_t is the atomic Gaussian radius after falling time t. The temperature of atoms in Red MOT is about 2μK consequently. Besides, on the basis of the fluorescent intensity detected by a photomultiplier tube (PMT), the number of the trapped atoms is measured and it is 1×10^7.

3　Realization of trapped cold Sr atoms in an optical lattice

3.1　Trap depth of an optical lattice

For the one-dimensional optical lattice, the electric fields of the two laser beams counter-propagating in the z direction can be expressed as

$$E = E_0\cos(kz-\omega t)+E_0\cos(-kz-\omega t), \tag{2}$$

here k is the wave vector of the laser, ω is the angular frequency. E_0 is the amplitude of the laser field. The 1-D lattice is experimentally shown in figure 3.

Fig. 3　Schematic setup of 1-D optical lattice

The laser beam is focused to a minimum beam waist by the lens1 and after propagating some distance, the beam passes through the lens 2 and is reflected without polarization rotation by a High Reflected (HR) mirror. By adjusting the HR mirror finely, we make sure the returning laser beam overlaps the incident one. The beam shows a Gaussian distribution, and in the longitudinal direction the potential energy can be described as below

$$U = 4U_0\exp\left[\frac{-2r^2}{\omega(z)^2}\right]\cos^2(2\pi z/\lambda_L). \tag{3}$$

The potential energy at the trap focus $[U]$ is obtained

$$[U] = -\frac{1}{4}\alpha|E_0|^2 = -\alpha\frac{4P}{c\varepsilon_0\pi\omega_0^2}, \tag{4}$$

where $E_0=\sqrt{\frac{2I\mu_0 C}{n}}$ (for air, the index of refraction $n=1$); α is the dipole polarizability related to the two clock states, P denotes the power of the single beam lattice laser, ω_0 is the beam waist at a longitudinal distance z. The trapping wells longitudinal dimension yielding vibration frequency ν_z at the trap waist ($z=0$, $r=0$), $\nu_z=\frac{1}{\lambda_L}\sqrt{\frac{2[U)]}{m}}$, for radial dimension $\nu_r=\frac{1}{\pi\omega_0}\sqrt{\frac{[U]}{m}}$, r is the radial distance and λ_L is the wavelength of the lattice laser.

Experimentally, the lattice laser is an External-Cavity Diode Laser (ECDL) operating at the "magic wavelength". The frequency- tuned rang of lattice laser can be up to 17GHz without mode-hop. An 813nm laser beam outputs from a single-mode fiber included in the laser, thus the space-mode of the laser beam can be optimized. The coupling efficiency of the fiber is about 65%. Finally the power 850mW at lattice wavelength 813nm isobtained and the laser beam is focused to a beam of 38 μmradius, corresponding to laser intensity 37.5kW/cm^2. As can be seen in Figure 4(a), Smaller the beam radius is, higher the intensity of the laser. Together with the calculated atomic polarization around λ_{magic}, the trap depth is estimated to be 570 E_R (about 95μK), where $E_R=\frac{(\hbar k)^2}{2m}$ is the recoil energy, m is the atomic mass (for Sr, $m=1.44\times10^{-25}$), $\hbar$ is the plank constant. The recoil shift ($\frac{E_R}{h}$) is 3.5 kHz. Figure 4(b) demonstrates the beam radius and its corresponding trap depth varying with the location z in the longitudinal direction. Based on the known value of trap depth, the expected vibration frequencies in the center of lattice are 166 kHz longitudinally and 800Hz radially. The clock transition can be probed along the longitudinal direction without the Doppler shift and recoil shift for its strong confinement.

3.2　Intensity noise of lattice laser—813nm

For the ECDL 813 nm laser, its intensity noise can deeply affect energy shift of atoms in the optical lattice.

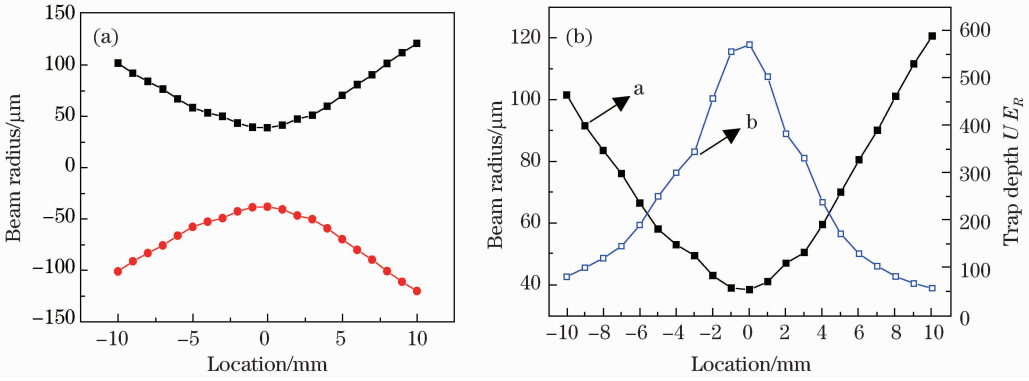

Fig. 4 Beam radius and trap depth varying with location z along longitudinal direction. (a) Relation of beam radius and location z; (b) line a is beam radius changing with location z and line b is trap depth changing with z

Heating cold atoms can be produced due to intensity fluctuations of the 813nm laser generating the optical lattice[23]. It is desirable to suppress the intensity noise to the shot noise limit (SNL). A very high finesse filter cavity (called Mode-cleaner)[24] is an effective tool to reduce the noise to SNL, which is also widely used for spatial cleaning of laser beams. Hence, a super-stable and high finesse filter is employed. The structure of the mode-cleaner is shown in figure 5, composed of 3 mirrors. M_1 and M_2 are flat mirrors whose reflectivity is 99.67% for 813 nm and M_3 is flat-curve mirror whose reflectivity is 99.93%. The curve radius of mirror M_3 is 1000 mm. The whole length of the Mode-cleaner is 430 mm, l_1 is 30mm and l_2 is the same to l_3 which is 200 mm.

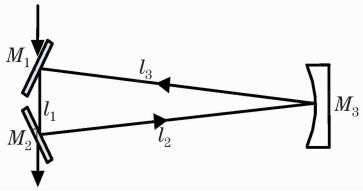

Fig. 5 Structure of mode-cleaner

According to the parameters of this mode-cleaner referred above, its beam waist is calculated theoretically by the ABCD transform matrix and the waist is $\omega_M = 327.5$ μm. The laser beam waist measured is 112 μm. Based on the known beam waists of the mode-cleaner and the laser beam outputting from 813nm diode laser, the parameter of the matching lens is calculated theoretically utilizing the transforming regulation of a gauss beam propagating through a lens. The reflected spectrum and transmitted spectrum are obtained when the optical mode is matched between them. The mode-cleaner is locked frequently by introducing the optical feedback on the basis of the PDH technology, then the cavity and the laser achieve to their resonance. Consequently, the intensity noise is measured by a pair of balanced photodiodes, reaching to SNL about at 8MHz. While the intensity noise of 813nm laser not filtered by the mode-cleaner cannot reach to the SNL within the analysis frequency 30MHz. The result is presented in figure 6. The level of noise suppression can allow the 813nm diode laser to be utilized in loading Sr cold atoms into the optical lattice without disturbance, which is also good at probing the signal of clock transition. It has not been used yet to the optical lattice in this paper that suppression of the intensity noise of 813nm laser. This will be applied to our experiment and optimize the optical lattice.

3.3 Cold Sr atoms confined in 1-D optical lattice

We choose one path passes through the atomic center and there is two counter-propagating beams, which is completed by a high-reflected plane mirror (99.5% reflectivity for 813 nm) as shown in figure 7. The laser beam output from the fiber is focused to 38μm by a lens whose focus length is 200 mm. This lens is located in front of a vacuum chamber and the focused beam waist overlaps rightly with the center of the atoms. After propagating a distance (about 400 mm between the two same lenses), the beam travels through another lens (f=200 mm) on the

other side of this chamber.

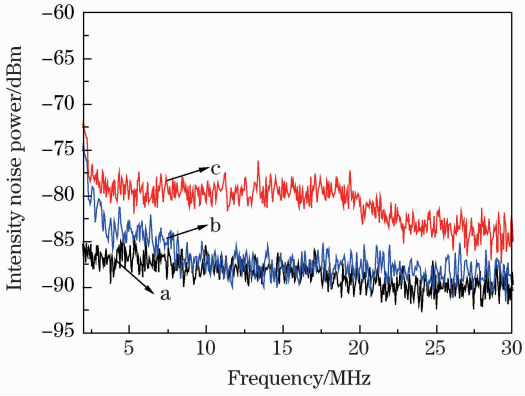

Fig. 6　Spectrums of intensity noise of 813 nm laser. Line *a* is shot noise limit; line *b* is spectrum when 813 nm laser passes through mode-cleaner; line *c* is spectrum when 813 nm laser does not pass through mode-cleaner

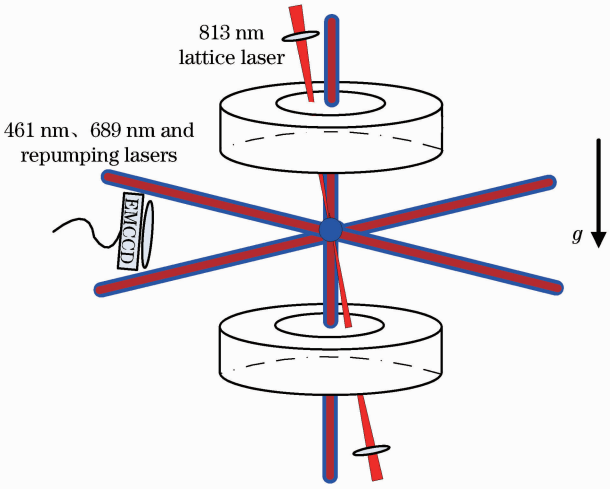

Fig. 7　Laser system for 1-D optical lattice

It is realized by the time sequence controlling of the lasers and magnetic field for the optical lattice, as shown in figure 8.

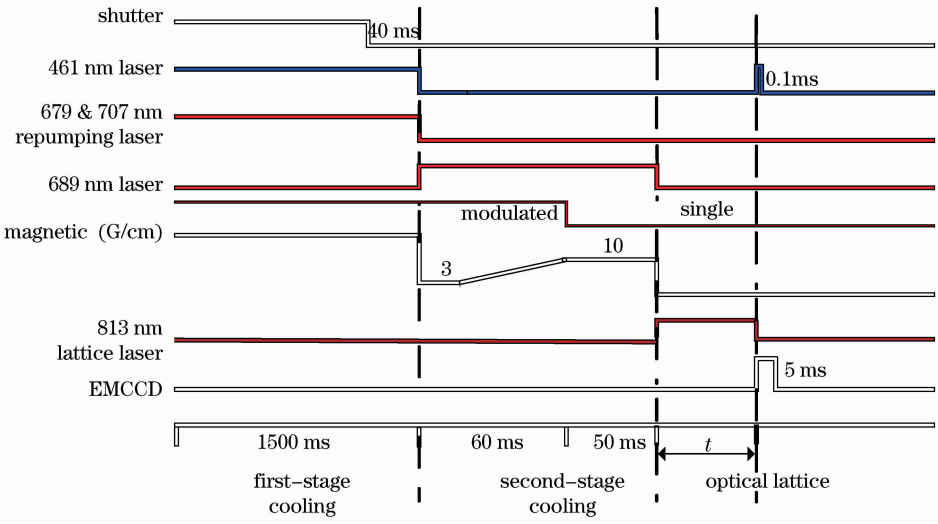

Fig. 8　Time sequence for 1-D optical lattice

After the realization of the cold atoms with μK temperature, all of the cooling lasers (461, 679, 707 and 689 nm) and the magnetic field are turned off. The 813nm laser is turned on and is kept on until the realization of the 1-D optical lattice. After a time-length *t*, a pulsed 461nm laser with band-width 0.1ms is

turned on to probe the trapped atoms. Simultaneously an EMCCD is trigged to monitor the images. Figure 9 is the fluorescent images of atoms trapped in the 813 nm lattice. As shown in figure 9, atoms are maintained in the same position varying with time t from 0 to 700 ms, (a) t=0 ms, (b) t=200ms, (c) t=400 ms, (d) t=700 ms, different from the dipole trap referred above. The bright zone in picture 9(a) is the cold atomic cloud, which falls down due to the gravity. Ideally the trapping force formed by the lattice laser is large enough to conquer the gravity influence on them. Although the ideal force traps these motional atoms in the same position for a long time, the brightness of trapped atoms displayed in figure 9 become weaker when time t postpones, which manifests the variance of the trapped atom number in 813 nm lattice. The number of atoms trapped in the 1-D optical lattice is estimated to be 1.2×10^5 by detecting the fluorescent intensity of atoms by the PMT.

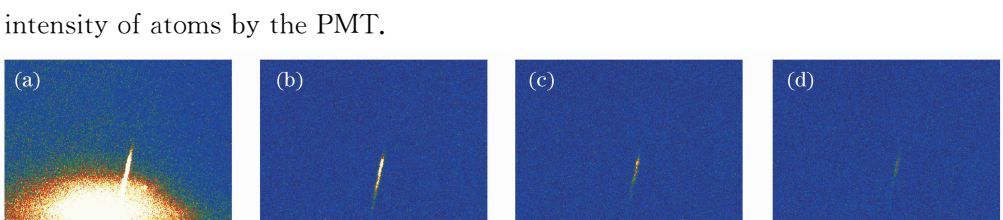

Fig. 9　Images of trapped atoms in 1-D optical lattice. (a) t=0 ms; (b) t=200 ms; (c) t=400 ms; (d) t=700 ms

Figure 10(a) is the lifetime of lattice based on the continuous variance of fluorescent intensity of atoms trapped in the optical lattice. The result of lifetime is about 270ms consequently. Figure 10(b) is the temperature of trapped atoms obtained by the method TOF. As can be seen, the value is about 3.5μK and there is no obvious influence of the power on the temperature. In all, this original and special approach by which atoms is trapped in the optical lattice can provide a long interrogation time for probing the clock transition, furthermore make the foundation for developing the optical lattice clock of Sr atoms.

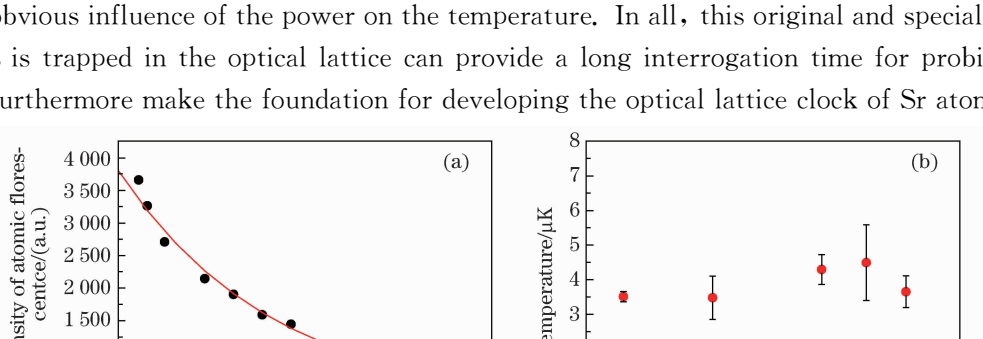

Fig. 10　Lifetime of trapped atoms in optical lattice and their temperature. (a) Atomic fluorescent intensity in 1-D optical lattice varying with time t; (b) temperature of atoms as a function of single lattice laser power

4　Conclusion

At present, the performance of optical lattice clocks surpass that of atomic fountains with the uncertainty and stability 10^{-18} level. Many research teams in the world work on Sr optical lattice clocks. For our laboratory, the cold atoms of Sr have been obtained with the temperature as low as 2μK and the number 1×10^7. However, the cold atoms cann't be used to obtain the clock transition directly because of the serious Doppler shift and the recoil shift. The optical lattice, a tight confinement is applied to control atoms' motion in range of the half wavelength. In our experiment, bosonic ^{88}Sr atoms are trapped in the 1—D optical lattice operating on the "magic" wavelength for the clock transition $(5s5s)^1S_0$—$(5s5p)^3P_0$,

with the lifetime 270ms. The next step is to probe the clock transition of ^{88}Sr. Considered that ^{88}Sr is boson, doubly-forbidden for $(5s5s)^1S_0$—$(5s5p)^3P_0$, a magnetic field is applied to stimulate the weak transition between them.

References

1 Takamoto M, Hong F L, Higashi R, *et al*.. An optical lattice clock [J]. Nature, 2005, 435(7040): 321-324.

2 Falke S, Lemke N, Grebing C, *et al*.. A strontium lattice clock with 3×10^{-17} inaccuracy and its frequency [J]. New J Phys, 2014, 16(7): 073023.

3 Gurov M, McFerran J J, Nagórny B, *et al*.. Optical lattice clocks as candidates for a possible redefinition of the SI second [J]. IEEE Trans Instrum Meas, 2013, 62(6): 1568—1573.

4 Hinkley N, Sherman J A, Phillips N B, *et al*.. An atomic clock with 10^{-18} instability [J]. Science, 2013, 341(6151): 1215—1218.

5 Huntemann N, Okhapkin M, Lipphardt B, *et al*.. High-accuracy optical clock based on the octupole transition in $^{171}Yb^+$ [J]. Phys Rev Lett, 2012, 108(9): 090801.

6 Margolis H S, Godun R M, Gill P, *et al*.. International timescales with optical clocks (ITOC) [C]. European Frequency and Time Forum & International Frequency Control Symposium, 2013: 908—911.

7 Chou C W, Hume D B, Koelemeij J C J, *et al*.. Frequency comparison of two high-accuracy Al^+ optical clocks [J]. Phys Rev Lett, 2010, 104(7): 070802.

8 Bloom B J, Nicholson T L, Williams J R, *et al*.. An optical lattice clock with accuracy and stability at the 10^{-18} level [J]. Nature, 2014, 506(7486): 71—75.

9 Jaksch D, Bruder C, Cirac J I, *et al*.. Cold bosonic atoms in optical lattices [J]. Phys Rev Lett, 1998, 81(15): 3108—3111.

10 Derevianko A, Katori H. Colloquium: physics of optical lattice clocks [J]. Rev of Mod Phys, 2011, 83(2): 331—347.

11 Wilpers G, Oates C W, Diddams S A, *et al*.. Absolute frequency measurement of the neutral 40Ca optical frequency standard at 657nm based on microkelvin atoms [J]. Metrologia, 2007, 44(2): 146—151.

12 Degenhardt C, Stoehr H, Lisdat C, *et al*.. Calcium optical frequency standard with ultracold atoms: approaching 10^{-15} relative uncertainty [J]. Phys Rev A, 2005, 72(6): 062111.

13 Itano W M, Bergquist J C, Bollinger J J, *et al*.. Quantum projection noise: population fluctuation in two-level systems [J]. Phys Rev A, 1993, 47(5): 3554—3570.

14 T Rosenband, D B Hume, P O Schmidt, *et al*.. Frequency ratio of Al^+ and Hg^+ single-ion optical clocks; metrology at the 17th decimal place [J]. Science, 2008, 319(5871): 1808—1812.

15 P Lemond. Optical lattice clock [J]. Eur Phys J Special Topics, 2009, 172(1): 81—96.

16 H Katori. Spectroscopy of strontium atoms in the Lamb-Dicke confinement [C]. Proceedings of the 6th Symposium on Frequency Standards and Metrology, 2002: 323-330.

17 Tian Xiao, Chang Hong, Wang Xinliang, *et al*.. Trapping four isotopes of strontium in a MOT by using Zeeman slowing [J]. Acta Optica Sinica, 2010, 30(3): 898—902.
田晓,常宏,王心亮,等. 利用塞曼减速法实现锶同位素的磁光阱俘获[J]. 光学学报, 2010, 30(3): 898—902.

18 Liu Hui, Ren Jie, Tian Xiao, *et al*.. Realization of narrow linewidth fluorescence spectrum of Strontium intercombination transition and analysis of its line broadening factors[J]. Acta Optica Sinica, 2013, 33(6): 0630001.
刘辉, 任洁, 田晓, 等. 锶原子窄线宽互组跃迁荧光谱获得及谱线增宽因素分析[J]. 光学学报, 2013, 33(6): 0630001.

19 Zhang Yin, Wang Qing. Research of automatic frequency stability diode laser [J]. Chinese J Lasers, 2014, 41(6): 0602001.
张胤,王青. 自动稳频半导体激光器研究[J]. 中国激光,2014,41(6): 0602001.

20 Yun Long, Zhuanxian Xiong, Xi Zhang, *et al*.. Frequency locking of a 399-nm. laser referenced to fluorescence spectrum of an ytterbium atomic beam[J]. Chin Opt Lett, 2014, 12(2): 021401.

21 Ma Weiguang, Zhao Gang, Fu Xiaofang, *et al*.. Stability analysis of fiber electro-optic modulator based PDH frequency locking technique [J]. Chinese J Lasers, 2014, 41(1):0115002.
马维光,赵刚,付小芳,等. 基于光纤电光调制器的PDH频率锁定稳定性研究[J]. 中国激光,2014,41(1):0115002.

22 Brzozowski T M, Maczynska M, Zawada M, *et al*.. Time-of-flight measurement of the temperature of cold atoms for short trap-probe beam distances [J]. J Opt B: Quantum Semiclass Opt, 2002, 4(1): 62—66.

23 Pichler H, Schachenmayer J, Daley A J, *et al*.. Heating dynamics of bosonic atoms in a noisy optical lattice [J]. Phys Rev A, 2013, 87(3): 033606.

24 Willke B, Uehara N, Gustafson E K, *et al*.. Spatial and temporal filtering of a 10-W Nd:YAG laser with a Fabry-Perot ring-cavity premode cleaner[J]. Opt Lett, 1998, 23(21):1704—1706.

栏目编辑: 刘丰瑞